# Nonlinear Analysis of Phase Relationships in Quasi-Optical Oscillator Arrays

R. A. York, *Member, IEEE*

*Abstract*—**A dynamic theory of coupled oscillators is developed and applied to the class of loosely-coupled quasi-optical oscillator arrays. This theory permits the calculation of stable, steady-state phase relationships between the oscillators. The distribution of free-running frequencies and the coupling parameters are most important in determining the behavior of the arrays. It is found that free-running frequencies of the peripheral elements have the strongest influence on the steady-state phase relationships. The influence of randomness in the frequency distribution is considered for the case of broadside beamforming, establishing a critical value for the coupling strength in order to maintain mutual synchronization with a specified maximum beam deviation. Techniques for simplifying the calculation of phase relationships for some common coupling parameters are also developed. The theory is supported by new experiments and other published results.**

## I. Introduction

QUASI-OPTICAL power-combining is a promising technique for overcoming the inherent power limitations of solid-state devices at millimeter-wave frequencies [1], particularly in light of recent experimental results using both two- and three-terminal devices [2]–[7]. Such arrays attract interest for several reasons: they can accommodate large numbers of devices and hence provide power levels which have traditionally required bulky vacuum-tube devices; high combining efficiencies are achieved by combining power in free-space; good reliability and DC-to-RF conversion efficiency are possible by virtue of the semiconductor devices; they can be fabricated compactly with existing monolithic technology, so that low cost arrays might be possible for high volume applications; and the arrays degrade gracefully, in contrast to vacuum-tube sources.

Regardless of the topology, all oscillator arrays must satisfy two key requirements: the devices must synchronize to a common frequency, and must maintain a desired phased relationship in the steady-state. The former is accomplished by coupling the devices together or to an external source, and relies on the phenomenon of injection-locking [35]–[37]. In practice, ensuring the proper phase relationship is most challenging. For the special case of identical unit cells [4], [7], a certain phase-distribution can be assumed and the proper conditions for preserving this distribution can be determined. However, this does not guarantee that such a phase distribution is stable, or that it will persist in a real array when the identical unit-cell assumption is invalid. Determining the phase relationships in free-running arrays requires a dynamic analysis of the nonlinear interactions between devices. A dynamic description of the arrays is also required to investigate the stability of different modes, transient effects, modulation and locking to external signals [5], and noise properties of the arrays [36].

Considering that a single nonlinear oscillator is difficult to analyze, a description of the dynamics of a large system of oscillators may seem hopelessly complicated. However, theoretical efforts in the mathematics community [21]–[31] have shown that much of the macroscopic behavior of coupled nonlinear systems can be described by relatively simple models. This paper describes a similar dynamic theory based on coupled Van der Pol equations, and applied to arrays of loosely coupled oscillators. Such arrays were among the first to be examined both experimentally [8] and theoretically [9]–[10] for use as quasi-optical power-combiners, and many suitable active antenna designs have been reported for these arrays [14]–[20]. Coupled-oscillator arrays have also recently been mode-locked for pulse generation [11]–[12], and exhibit interesting beam-scanning properties [12]–[13]. The theory presented in this paper can be used to determine the steady-state phase relationships in these arrays, and to investigate other dynamic effects. The theory is applied to some cases of interest for practical quasi-optical power-combining, including broadside beamforming, random frequency distributions, and electronic beam-scanning. Some experimental results are then described which examine the influence of coupling parameters on the phase distribution.

## II. Coupled Oscillator Theory

The theory of coupled nonlinear oscillators is the subject of increasing research activity, due to successful modelling of many diverse biological and physical phenomena. Examples include swarms of synchronously flashing fireflies [21], the coordinated firing of cardiac pacemaker cells [22], rhythmic spinal locomotion in vertebrates [23]–[24], the synchronized activity of nerve cells in response to external stimuli [21], and synchronized menstrual cycles in groups of women [25]. In the physical sciences, examples include oscillations in certain nonlinear chemical reactions [26], the collective behavior of Josephson junction arrays [27]–[28], and laser diode arrays. Almost any system of discrete or distinguishable units that collectively exhibit macroscopic synchronous behavior can be

Manuscript received September 9, 1992; revised March 30, 1993. This work was supported in part by the U.S. Army Research Office under contract DAAL03-89-K-0041.

The author is with the Department of Electrical Engineering, University of California at Santa Barbara, Santa Barbara, CA 93106

IEEE Log Number 9211935.

modelled by a system of coupled oscillators. This is apparently true even when the oscillators and/or the mechanisms for coupling between them are not understood in great detail.

As Koppel [24] suggests, ". . . the behavior of oscillators, when forced or coupled to other systems, is relatively insensitive to the detailed description of the oscillators themselves or the coupling." Indeed, the present author's experimental work with coupled microwave oscillators has shown this to be the case. The oscillators alternately used Gunn, IMPATT, and MESFET devices, and despite the significantly different physical mechanisms responsible for the negative resistance and gain saturation in each device, the oscillators behaved similarly when coupled together. These observations suggest that any simple model which is capable of generating sinusoidal oscillations might adequately represent the individual oscillators in a coupled system. One such model is the Van der Pol equation [32], which is taken in the following sections to represent a generic microwave oscillator. A similar phenomenological approach will also be adopted to describe the mutual coupling between the oscillators in an array, rather than focus on a specific physical mechanism. In this way the following analyses may prove useful in describing the dynamics of other types of quasi-optical oscillator arrays [4], [7].

### A. Oscillator Modelling

Many narrowband microwave oscillators can be represented by the simple circuit shown in Fig. 1. The active device is modelled by a lumped negative resistance (conductance), which is embedded in a series (parallel) resonant circuit; any reactive component of the device impedance is considered part of the embedding network. The negative resistance $R_d(|V|)$ is assumed independent of frequency, but must depend nonlinearly on the amplitude of oscillation. The circuit equation for Fig. 1 is

$$\frac{dV}{dt} + \omega_0^2 \int V\,dt + V\,\frac{\omega_0}{Q}\left[1 - \frac{R_d(|V|)}{R_L}\right] = \frac{\omega_0}{Q}\,V_{\text{inj}} \quad (1)$$

where $\omega_0$ is the resonant frequency of the circuit, $V$ is the complex (phasor) output voltage, $Q$ is the $Q$-factor of the embedding network, and $V_{\text{inj}}$ represents any externally injected signals. The $Q$-factor is sufficiently high ($Q > 10$) so that the oscillator frequency will remain close to $\omega_0$, and therefore the amplitude and phase terms will be slowly varying functions of time (compared with the period of oscillation). The output voltage can then be written as

$$V = A(t)e^{j(\omega_0 t + \phi(t))} = A(t)e^{j\theta(t)} \quad (2)$$

where $A$ is the amplitude of oscillation, and $\theta$ is the instantaneous phase. The integral in (1) can be integrated by parts to give [37]

$$\int V\,dt = \frac{-2jV}{w_0} + \frac{1}{w_0^2}\frac{dV}{dt} + \cdots. \quad (3)$$

Higher order terms can be neglected under the assumption of slowly varying parameters. Following Van der Pol [32], the device saturation is modelled by a quadratic such that

$$1 - R_d/R_l \simeq \mu\left(\alpha_0^2 - |V|^2\right) \quad (4)$$

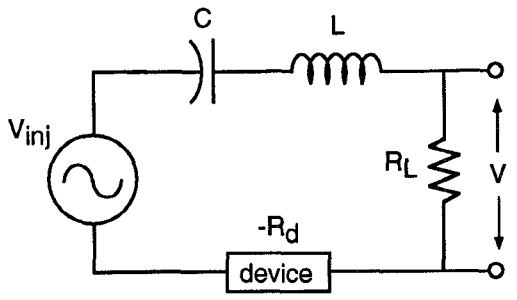


Fig. 1. Simple model for narrowband microwave oscillators. The device negative resistance is a function of the amplitude of oscillation, $V$, and the voltage source $V_{\text{inj}}$ accounts for injected signals from neighboring oscillators.

where $\alpha_0$ is the free-running amplitude of oscillation, and $\mu$ is an empirical nonlinearity parameter describing the oscillator. This expression is consistent with the Barkhausen Criterion for oscillation. Substituting (3) and (4) into (1) gives a complex form for the forced sinusoidal Van der Pol model as

$$\frac{dV}{dt} = V\left[\frac{\mu\omega_0}{2Q}\left(\alpha_0^2 - |V|^2\right) + j\omega_0\right] + \frac{\omega_0}{2Q}\,V_{\text{inj}}. \quad (5)$$

Using (2), the amplitude and phase dynamics can be written separately as

$$\frac{dA}{dt} = \mu\,\frac{\omega_0}{2Q}\,A(\alpha_0^2 - A^2) + \frac{\omega_0}{2Q}\,A\,\text{Re}\left\{\frac{V_{\text{inj}}}{V}\right\} \quad (6a)$$

$$\frac{d\theta}{dt} = \omega_0 + \frac{\omega_0}{2Q}\,\text{Im}\left\{\frac{V_{\text{inj}}}{V}\right\} \quad (6b)$$

where Re{} and Im{} denote the real and imaginary parts of the bracketed expression, respectively.

### B. Adler's Equation

For low-level injected signals such that $|V_{\text{inj}}| \ll |V|$, the oscillator amplitude will remain close to its free-running value. Excluding an initial turn-on transient, the dynamic behavior of the system is then governed predominantly by the differential equation for the phase variables (6b). Writing

$$V_{\text{inj}} = A_{\text{inj}}e^{j(\omega_{\text{inj}}t + \psi_{\text{inj}})} = A_{\text{inj}}e^{j\theta_{\text{inj}}}$$

and substituting in (6b) gives

$$\frac{d\theta}{dt} = \omega_0 + \frac{\omega_0}{2Q}\frac{A_{\text{inj}}}{A}\sin(\theta_{\text{inj}} - \theta) \quad (7)$$

which is a form of Adler's equation for injection-locking [35]–[36]. When the oscillator locks onto the injected signal, $d\theta/dt = \omega_{\text{inj}}$ in the steady-state, and (7) becomes

$$\omega_{\text{inj}} - \omega_0 = \Delta\omega_{lock}\sin\Delta\theta$$

$$\text{where } \Delta\omega_{lock} = \frac{\omega_0}{2Q}\frac{A_{\text{inj}}}{A} \quad (8)$$

$\Delta\omega_{lock}$ is called the *locking bandwidth* of the oscillator, and $\Delta\theta$ is the steady-state phase difference between the oscillator and injected signal. Equation (8) indicates that as the injected signal frequency is tuned over the locking range of the oscillator, $\omega_0 \pm \Delta\omega_{lock}$, the phase difference will vary between $-90° < \Delta\theta < 90°$. Critics of the coupled-oscillator architecture initially cited this latter result as a serious drawback,

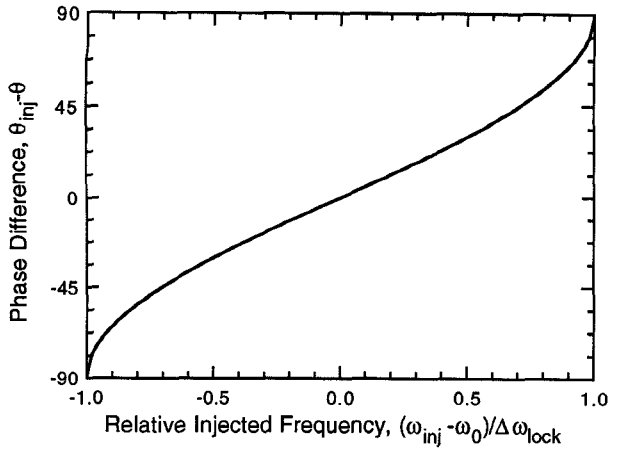


Fig. 2. Phase difference between the injected signal and oscillator output as a function of the injected frequency, according to Adler's equation (8).

because of the implication that any statistical discrepancies in the oscillator free-running frequencies could produce large phase-shifts in the array, which would reduce the power-combining efficiency. However, as shown in Fig. 2, much of this phase variation occurs for frequency shifts near the edge of the locking range. Furthermore, the situation in coupled arrays is more fortuitous, because there is a *mutual* interaction between the oscillators rather than the unilateral injection described above, and because each oscillator is coupled to more than one neighboring oscillator. The net result is that such phase shifts tend to average out for random frequency distributions, provided that the frequencies do not fluctuate too violently. On the other hand, these phase-shifts could also be exploited for the purpose of electronic beam-scanning. These topics will be explored in a later section.

### C. Loosely-Coupled Sinusoidal Oscillators

For a system of coupled oscillators, the mutual interaction between oscillators $i$ and $j$ is described by a complex coupling coefficient, $\kappa_{ij}$, which has a magnitude and phase given by

$$\kappa_{ij} \equiv \varepsilon_{ij} e^{-j\Phi_{ij}} .$$

In most arrays, reciprocity will hold so that $\kappa_{ij} = \kappa_{ji}$. This coupling parameter is unitless and defined such that in a system of $N$ oscillators, the injected signal at the $i$th oscillator can be written as

$$V_{\text{inj}} = \sum_{j=1}^{N} \kappa_{ij} V_j \tag{9}$$

where $V_i$ is the complex (phasor) output voltage of the $i$th oscillator. For some types of coupling, such as radiative interaction between antennas or transmission-line coupling circuits, the $\kappa_{ij}$ can be directly related to commonly used $N$-port network parameters. In other cases where the coupling mechanism is significantly more complicated or not well understood, such as coupling through the modes of an external cavity, this modelling approach can be considered phenomenological. In either case, simple experiments can be performed to determine the coupling parameters for a particular system [43]. Using (9) and (5), the system dynamics are described by

$$\frac{dV_i}{dt} = V_i \left[ \frac{\mu\omega_i}{2Q} \left( \alpha_i^2 - |V_i|^2 \right) + j\omega_i \right] + \frac{\omega_i}{2Q} \sum_{j=1}^{N} \kappa_{ij} V_j \qquad i = 1, 2, \cdots, N \tag{10}$$

where the subscript $i$ denotes the $i$th oscillator. For simplicity, it is assumed that all of the oscillators have approximately the same $Q$- and $\mu$-factors. Writing $V_i = A_i e^{j\theta_i}$ enables the amplitude and phase dynamics to be separated as

$$\frac{dA_i}{dt} = \frac{\mu\omega_i}{2Q} \left( \alpha_i^2 - A_i^2 \right) A_i + \frac{\omega_i}{2Q} \sum_{j=1}^{N} \varepsilon_{ij} A_j \cos(\Phi_{ij} + \theta_i - \theta_j) \tag{11a}$$

$$\frac{d\theta_i}{dt} = \omega_i - \frac{\omega_i}{2Q} \sum_{j=1}^{N} \varepsilon_{ij} \frac{A_j}{A_i} \sin(\Phi_{ij} + \theta_i - \theta_j) \qquad i = 1, 2, \cdots, N . \tag{11b}$$

When $\varepsilon_{ij} = 0$, the oscillators are uncoupled and (11) reduces to a set of independent sinusoidal oscillators with amplitudes $A_i = \alpha_i$ and frequencies $\omega_i$. These coupled, nonlinear equations are impossible to solve analytically in the general case of arbitrary coupling strength, and we must resort to computer simulations. However, considerable simplification of (11) occurs in the limit of weak coupling, where $\varepsilon_{ij} \ll 1$. The amplitudes of the oscillators will then remain close to their free-running values ($A_i \approx \alpha_i$), and the phase dynamics of the system will be described predominantly by

$$\frac{d\theta_i}{dt} = \omega_i - \frac{\omega_i}{2Q} \sum_{j=1}^{N} \varepsilon_{ij} \frac{\alpha_j}{\alpha_i} \sin(\Phi_{ij} + \theta_i - \theta_j) \qquad i = 1, 2, \cdots, N . \tag{12}$$

Because of the similarity in form and approximations used, (12) can be viewed as a generalization of the Adler equation (7). This equation is the basis for the coupled-oscillator theory in this paper. Although (12) only strictly applies in the limit of weak coupling, many of the conclusions reached in subsequent discussions can be expected to hold far from this limit, at least approximately [24]. This is true in the present case because the amplitude dynamics have only a second-order influence on the phase dynamics, which are fundamentally more important to the operation of practical oscillator arrays.

Under certain conditions all of the oscillators will become synchronized to a common frequency $\omega$, so that $d\theta_i/dt = \omega$ for all $i$. The steady-state frequency and phase distribution can then be found by solving

$$\omega = \omega_i \left[ 1 - \frac{1}{2Q} \sum_{j=1}^{N} \varepsilon_{ij} \frac{\alpha_j}{a_i} \sin(\Phi_{ij} + \theta_i - \theta_j) \right] \qquad i = 1, 2, \cdots, N . \tag{13}$$

One of the phase variables is arbitrary and can be set to zero, so (13) describes a set of $N$ equations with $N$ unknowns. As discussed in [43], the self-interaction term, $\varepsilon_{ii}$, is not

necessarily zero. A non-zero $\varepsilon_{ii}$ can be used to model the influence of external feedback elements such as quasi-optical reflectors positioned above the array. However, it is always possible to define a new free-running frequency, $\tilde{\omega}_i$, to account for this term, where

$$\tilde{\omega}_i = \omega_i \left[1 - \frac{\varepsilon_{ii}}{2Q} \sin \Phi_{ii}\right].$$

Therefore, the following discussions assume that $\varepsilon_{ii} = 0$.

### D. Linear Arrays with Nearest-Neighbor Coupling

In most conceivable quasi-optical arrays, each oscillator will interact locally with other oscillators within some finite region surrounding the oscillator. An exception is when the array is placed in a Fabry–Perot cavity [1], in which case there is a global, or "all-to-all" coupling. This problem has been treated using methods of statistical physics [26]–[27]. In the majority of cases, however, nearest-neighbor coupling dominates. In the following, we will consider linear chains of oscillators with nearest-neighbor coupling described by

$$\kappa_{ij} = \begin{cases} \varepsilon e^{-j\Phi} & \text{if } |i-j| = 1 \\ 0 & \text{otherwise} \end{cases}. \tag{14}$$

Fig. 3 illustrates such a system, where each oscillator is coupled to an antenna. Substituting this expression into (12) gives

$$\frac{d\theta_i}{dt} = \omega_i - \frac{\varepsilon\omega_i}{2Q} \sum_{\substack{j=i-1 \\ j\neq 1}}^{i+1} \frac{\alpha_j}{\alpha_i} \sin(\Phi + \theta_i - \theta_j)$$
$$i = 1, 2, \cdots, N \tag{15}$$

where $\alpha_0 = \alpha_{N+1} \equiv 0$. Since we are primarily interested in the case when the oscillators can mutually lock, another useful simplification can be made by defining

$$\Delta\omega_m \equiv \frac{\varepsilon\omega_i}{2Q}. \tag{16}$$

By comparison with (8), $\Delta\omega_m$ can be interpreted as the locking range of the $i$th oscillator when all the amplitudes are identical. Since the free-running frequencies $\omega_i$ must be close in value on the order of $\Delta\omega_m$ for locking to occur, then we can take $\Delta\omega_m$ to be the same for all oscillators and write (15) as

$$\frac{d\theta_i}{dt} = \omega_i - \Delta\omega_m \sum_{\substack{j=i-1 \\ j\neq i}}^{i+1} \frac{\alpha_j}{\alpha_i} \sin(\Phi + \theta_i - \theta_j)$$
$$i = 1, 2, \cdots, N. \tag{17}$$

This simplification amounts to ignoring any second-order variations in frequency and phase. In some cases, such as mode-locked arrays [11]–[12], the frequency differences are large enough to invalidate this assumption, and (15) must be used.

Equations (15) or (17) can be cast in a form involving relative phase shifts between adjacent oscillators. Defining

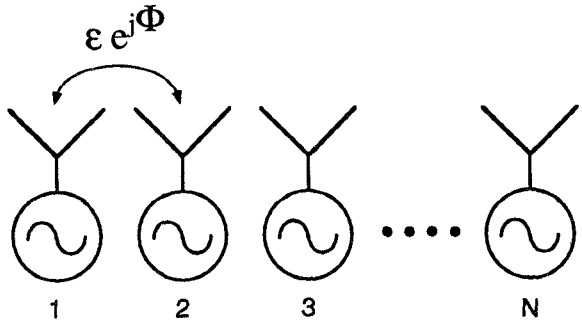


Fig. 3. Linear array of $N$ active antenna oscillators with nearest-neighbor coupling described by a coupling strength $\varepsilon$ and coupling angle $\Phi$.

$\Delta\theta_i = \theta_i - \theta_{i+1}$ and $\Omega_i = \omega_i - \omega_{i+1}$, and using (17) gives

$$\frac{d}{dt}\Delta\theta_i = \Omega_i - \Delta\omega_m H_i\left(\overline{\Delta\theta}\right)$$
$$i = 1, 2, \cdots, N-1$$
$$\text{where } H_i\left(\overline{\Delta\theta}\right) = \frac{\alpha_{i-1}}{\alpha_i} \sin(\Phi - \Delta\theta_{i-1}) + \frac{\alpha_{i+1}}{\alpha_i} \sin(\Phi + \Delta\theta_i) - \frac{\alpha_i}{\alpha_{i+1}} \sin(\Phi - \Delta\theta_i) - \frac{\alpha_{i+2}}{\alpha_{i+1}} \sin(\Phi + \Delta\theta_{i+1}) \tag{18}$$

and $\overline{\Delta\theta}$ is a vector with elements $\Delta\theta_i$. The steady-state solution for the phase distribution is then found by solving the set of equations

$$H_i\left(\overline{\Delta\theta}\right) = \frac{\Omega_i}{\Delta\omega_m} \qquad i = 1, 2, \cdots, N-1 \tag{19}$$

which can be accomplished with standard nonlinear root-finding algorithms [44]. Such solutions are called *fixed points* [38] of (18). Since the $H_i$ are bounded, periodic functions, there are generally no solutions to (19) unless the frequency differences $\Omega_i$ fall within some small range $|\Omega_i| \leq \Delta\omega_m H_{\max}$. If there are no solutions to (19) for a given set of $\Omega_i$, then mutual synchronization is impossible. When there are solutions, (17) can be used to find the steady-state frequency, $\omega$.

### E. Stability Analysis

When mutual synchronization is possible, there are usually $2^{N-1}$ different phase distributions, or modes, which satisfy (19). However, not all of these will be stable solutions. The stability of solutions to nonlinear equations such as (18) can be determined by linearizing the equation around its fixed points [38]. Assuming $\overline{\hat{\Delta\theta}}$ is a solution vector to (19), it is perturbed by letting $\Delta\theta_i = \Delta\hat{\theta}_i + \delta_i$, where the perturbation $\bar{\delta}$ is small such that

$$H_i\left(\overline{\hat{\Delta\theta}} + \bar{\delta}\right) \cong H_i\left(\overline{\hat{\Delta\theta}}\right) + \sum_{j=1}^{N-1} \frac{\partial H_i\left(\overline{\hat{\Delta\theta}}\right)}{\partial\Delta\theta_j} \delta_j. \tag{20}$$

Substituting (20) into (18), and using (19) gives the matrix equation

$$\frac{d\bar{\delta}}{dt} = \Delta\omega_m \overline{\overline{M}}\, \bar{\delta} \tag{21}$$

where $\bar{\delta}$ is a vector with elements $\delta_i$, and $\overline{\overline{M}}$ is an $(N-1)\times(N-1)$ stability matrix with elements

$$m_{ij} = -\frac{\partial H_i\left(\hat{\overline{\Delta\theta}}\right)}{\partial \Delta\theta_j}. \tag{22}$$

For the present case of nearest-neighbor coupling, $\overline{\overline{M}}$ is a tridiagonal matrix. A solution $\hat{\overline{\Delta\theta}}$ is stable with respect to small perturbations if the perturbation decays with time, which will occur when all of the eigenvalues of the stability matrix $\overline{\overline{M}}$ have negative real parts [39]. This requirement is so restrictive that nearly all of the solutions found from (19) will be eliminated.

In the general case when the assumption of nearest-neighbor coupling is invalid, or two-dimensional arrays are used instead of linear chains, a similar perturbation analysis can be performed using (12). However, since (12) is not conveniently described in terms of relative phases as in (18), the stability matrix will have dimensions $N\times N$, and one of the eigenvalues will always be zero. This is a result of the arbitrary assignment of a phase reference. A stable solution in that case corresponds to all but one of the eigenvalues having negative real parts [39].

## III. Important Results for Power-Combining Arrays

Practical application of oscillator arrays require certain phase distributions to be synthesized, and a knowledge of how a variation in free-running parameters will affect the array performance. A few such cases are considered here. For notational convenience, the following discussion assumes identical free-running amplitudes of the oscillators: $\alpha_i = 1$ for $i = 1, 2, \cdots, N-1$. However, the following analytical techniques can still be applied in cases where the effects of non-uniform amplitudes are important, such as applications requiring low radiation sidelobes, or other beam shapes that can be synthesized by amplitude tapering according to classical array theory [45].

### A. Conditions for Broadside Phases

The output power of the quasi-optical oscillator array must be concentrated in a single narrow beam, and focused in a predictable direction. Typically a broadside radiation pattern is desired, which is obtained by operating all elements in phase. This places restrictions on the coupling angle, $\Phi$, and the distribution of free-running frequencies, $\omega_i$. Consider a chain of $N$ oscillators with nearest neighbor coupling. Substituting the desired mode $\Delta\theta_i = 0$ into the governing equations (17) gives

$$\begin{aligned}
\omega &= \omega_1 - \Delta\omega_m \sin\Phi \\
\omega &= \omega_2 - 2\Delta\omega_m \sin\Phi \\
&\vdots \\
\omega &= \omega_{N-1} - 2\Delta\omega_m \sin\Phi \\
\omega &= \omega_N - \Delta\omega_m \sin\Phi .
\end{aligned} \tag{23}$$

These equations can be satisfied by the free-running frequency distribution

$$\omega_i = \begin{cases} \omega + \Delta\omega_m \sin\Phi & i = 1 \quad \text{or} \quad i = N \\ \omega + 2\Delta\omega_m \sin\Phi & \text{otherwise}. \end{cases} \tag{24}$$

For a given $\Phi$ and $\omega$, the in-phase mode is obtained by setting the central oscillators to a common frequency $\omega + 2\Delta\omega_m \sin\Phi$, and slightly raising or lowering the end elements' free-running frequencies. The stability matrix (22) for this mode ($\Delta\theta_i = 0$) becomes

$$\overline{\overline{M}} = \Delta\omega_m \cos\Phi \begin{pmatrix} -2 & 1 & & & 0 \\ 1 & -2 & 1 & & \\ & 1 & -2 & 1 & \\ & & & \ddots & \\ 0 & & & 1 & -2 \end{pmatrix}. \tag{25}$$

The matrix $\overline{\overline{M}}$ is real and symmetric, and therefore all eigenvalues are real [40]. Furthermore, if such a matrix is *negative-definite,* the eigenvalues will also be negative [40]. Since the matrix is diagonally dominant ($|m_{ii}| \geq \sum_{j=1, j\neq i}^{N} |m_{ij}|$), it will be negative-definite when all of the diagonal elements are negative [41], which occurs when $\cos\Phi > 0$. Therefore a stable, in-phase mode ($\Delta\theta_i = 0$) is only possible when $-90° < \Phi < 90°$. For values of coupling angle outside this range, a similar analysis shows that the frequency distribution (24) will enforce the mode $\Delta\theta_i = 180°$, producing an end-fire pattern.

In a simple array of identical oscillators with no provision for electronic or mechanical tuning of the oscillator frequencies, the above analysis indicates that the in-phase mode can only be obtained if the coupling angle is $\Phi = 0°$. However, in radiatively coupled arrays the coupling angle $\Phi$ is set by the antenna spacing [43], which is constrained to less than a wavelength to suppress grating lobes in the radiation pattern. In such cases it may be difficult to achieve $\Phi = 0°$, and a broadside pattern can only be obtained by adjusting the frequencies of the end elements of the array, as described above. The frequency distribution and coupling angles required for broadside radiation are shown in Fig. 4. The influence of the end elements' frequencies on the steady-state phase distribution is a peculiar feature of coupled-oscillator systems. It is also an attractive feature in planar arrays, since it is generally easier to provide for tuning circuitry on the array periphery (where space constraints are relaxed) than for central portions of the array.

### B. Analysis with Zero Coupling Phase

For arbitrary coupling phase, (17)–(19) must be solved numerically for the unknown phases and synchronized frequency, but for the special cases of $\Phi = 0°$ and $\Phi = 180°$ the equations reduce to a form which can be solved by conventional linear

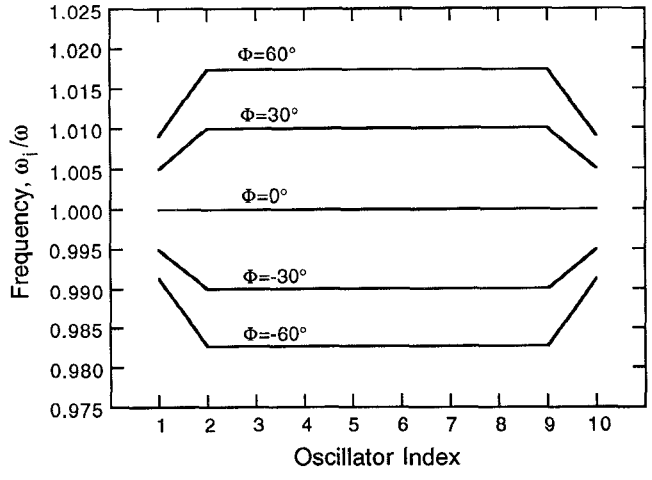


Fig. 4. Free-running frequency distributions required to achieve a stable broadside beam (identical phases) as a function of the coupling phase angle (24).

techniques. For $\Phi = 0°$, (18) become

$$\frac{d}{dt}\Delta\theta_i = \begin{cases} \Omega_1 + \Delta\omega_m[-2\sin\Delta\theta_1 + \sin\Delta\theta_2] \\ \quad i = 1 \\ \Omega_i + \Delta\omega_m[\sin\Delta\theta_{i-1} - 2\sin\Delta\theta_i + \sin\Delta\theta_{i+1}] \\ \quad i = 2\cdots N-2 \\ \Omega_{N-1} + \Delta\omega_m[\sin\Delta\theta_{N-2} - 2\sin\Delta\theta_{N-1}] \\ \quad i = N-1\,. \end{cases} \tag{26}$$

The $\sin\Delta\theta_i$ terms can now be considered independent variables. In the steady-state, (26) can be written as a matrix equation

$$\Delta\omega_m \overline{\overline{A}}\,\overline{S} = -\overline{\Omega} \tag{27}$$

where $\overline{S}$ and $\overline{\Omega}$ are $N-1$ vectors, and $\overline{\overline{A}}$ is a tridiagonal $(N-1)\times(N-1)$ matrix given by

$$\overline{S} = \begin{pmatrix} \sin\Delta\theta_1 \\ \sin\Delta\theta_2 \\ \vdots \\ \sin\Delta\theta_{N-1} \end{pmatrix} \quad \overline{\Omega} = \begin{pmatrix} \Omega_1 \\ \Omega_2 \\ \vdots \\ \Omega_{N-1} \end{pmatrix}$$

$$\overline{\overline{A}} = \begin{pmatrix} -2 & 1 & & 0 \\ 1 & -2 & 1 & \\ & & \ddots & \\ 0 & & 1 & -2 \end{pmatrix}.$$

The solution for the sine vector is of course

$$\overline{S} = -\frac{\overline{\overline{A}}^{-1}\overline{\Omega}}{\Delta\omega_m} \tag{28}$$

and the matrix $\overline{\overline{A}}$ has a simple inverse [23]

$$\left[\overline{\overline{A}}^{-1}\right]_{ij} = \frac{j(i-N)}{N} \qquad i \geq j$$

$$\left[\overline{\overline{A}}^{-1}\right]_{ij} = \left[A^{-1}\right]_{ji}.$$

Clearly there are no possible solutions of (28) if any element of the column vector $\overline{\overline{A}}^{-1}\overline{\Omega}$ has a magnitude greater than $\Delta\omega_m$. When there is a valid solution for the sine vector this will correspond to $2^{N-1}$ different solutions for the phase differences. The eigenvalues of the stability matrix must then be evaluated, where

$$\overline{\overline{M}} = \begin{pmatrix} -2\cos\theta_1 & \cos\theta_2 & & 0 \\ \cos\theta_1 & -2\cos\theta_2 & \cos\theta_3 & \\ & & \ddots & \\ 0 & & \cos\theta_{N-2} & -2\cos\theta_{N-1} \end{pmatrix}. \tag{29}$$

The stability constraint will remove all but one solution. For the case of $\Phi = 180°$, the same (27) is obtained, but both $\overline{\overline{A}}$ and $\overline{\overline{M}}$ have the opposite sign.

### C. Random Frequency Distributions

The problem of randomness in the frequency distribution is of considerable practical importance in quasi-optical oscillator arrays, since there will be inherent differences between devices and circuits as a result of manufacturing tolerances. This problem has been considered for some simple cases [26], [27], [31]. The techniques described in [31] can be applied to (17) for the case of nearest-neighbor coupling, identical amplitudes, and $\Phi = 0°$, and yields an estimate of the maximum "spread" of frequencies that such a system can tolerate before the phase distribution exceeds some specified worst case. With these assumptions, (17) becomes

$$\omega = \omega_i - \Delta\omega_m \sum_{\substack{j=i-1 \\ j\neq i}}^{i+1} \sin(\theta_i - \theta_j) \qquad i = 1, 2\cdots, N \tag{30}$$

in the steady-state. When all $N$ equations are added, the sine terms cancel to give

$$\omega = \frac{1}{N}\sum_{i=1}^{N}\omega_i\,. \tag{31}$$

That is, the final locked frequency is just the average of the free-running frequencies. Similarly adding the first $n$ equations of (30) gives

$$n\omega = \sum_{i=1}^{n}\omega_i + \Delta\omega_m \sin\Delta\theta_n \qquad n = 1, 2, \cdots, N-1\,. \tag{32}$$

Denoting the $n$th partial sum of frequencies by

$$Y_n = \sum_{i=1}^{n}\omega_i \tag{33}$$

then (32) becomes

$$-\Delta\omega_m \sin\Delta\theta_n = Y_n - \frac{n}{N}Y_N \qquad n = 1, 2, \cdots, N-1\,. \tag{34}$$

In the present case, identical free-running frequencies will produce a broadside radiation pattern. If the frequencies are

randomly distributed around this ideal, then a random phase distribution will result which generally shifts the beam away from broadside. Suppose that a worst-case scan angle of $\psi$ can be tolerated, corresponding to an average phase shift of $\Delta\phi_{\text{ave}}$. Equation (34) implies that this constraint can be satisfied if $\Delta\omega_m$ is greater than some critical value,

$$\Delta\omega_m \geq \text{Max}\left|\frac{Y_n - \frac{n}{N}Y_N}{\sin\Delta\phi_{\text{ave}}}\right| \qquad n = 1, 2, \cdots, N \qquad (35)$$

where $\text{Max}|\cdots|$ denotes the maximum value of the argument over the range of $n$. When $|\sin\Delta\phi_{\text{ave}}| = 1$, (35) provides a condition for mutual synchronization. The $Y_n$ define a random walk, so that the critical value for $\Delta\omega_m$ depends not only on the spread of free-running frequencies but also how they are arranged or distributed over the array. It has been shown that the "worst" distribution for a given set of frequencies is when they are arranged in order of increasing or decreasing frequency [31]. This fact can be used to determine the maximum tolerable frequency variation for a given locking range.

Fig. 5 shows the results of a numerical solution of (17) for 20 oscillators with a random frequency distribution centered around 10 GHz, and using a fourth-order Runga–Kutta routine [44]. In this simulation, a coupling strength of $\varepsilon = 0.1$ was chosen, with $Q = 10$, giving a locking range of $\Delta\omega_m \approx 50$ MHz. The oscillator frequencies shown in Fig. 5(a) were chosen with a random number generator, in the range $10 \pm 0.01$ GHz. The maximum value of the numerator in (35) is 21 MHz for this distribution, indicating that mutual synchronization will occur, with a maximum possible (worst case) average phase shift of $\Delta\phi_{\text{ave}} = \sin^{-1}(21/50) = 25°$, corresponding to a maximum scan angle deviation of $\psi = \pm 8°$ from broadside for half-wavelength spacing (36). Fig. 5(b) shows the array factor calculated from the steady-state phase distribution at the end of the simulation, and normalized to an ideal broadside pattern. The array factor clearly shows a single main lobe, and is well within the worst-case scan angle deviation predicted by the theory.

In their paper, Strogatz and Mirollo [31] also derive an expression for the "probability of locking" for one- and two-dimensional arrays with randomly distributed frequencies and nearest-neighbor coupling. They are able to show that for a fixed $\Delta\omega_m$, the probability that the array will lock to a single frequency tends to zero as the number of oscillators goes to infinity. This is primarily due to the assumption of nearest-neighbor coupling—as the array gets larger, it takes longer for elements on opposite ends of the array to communicate with each other. To ensure that mutual locking will occur, the coupling strength must increase at the rate of $\sqrt{N}$. That is, a 100-element linear array with random frequencies will require a coupling strength that is $\sqrt{10}$ times bigger than a 10-element linear array with random frequencies. This is also true for a two-dimensional array, but the required locking range is then reduced by a factor of 2 since each oscillator generally has twice as many nearest-neighbors.

The above analyses reinforce our intuition that a large locking bandwidth is desirable for each array element. This can be achieved by increasing the coupling strength, or decreasing the $Q$-factor of the individual oscillators. For large arrays, it may be necessary to place the array in a high-$Q$ Fabry–Perot cavity, which would effectively extend the oscillator interaction beyond nearest-neighbors and also increase the strength of the mutual coupling. However, this would reduce the modulation bandwidth of the array. This power-bandwidth tradeoff needs to be more carefully explored.

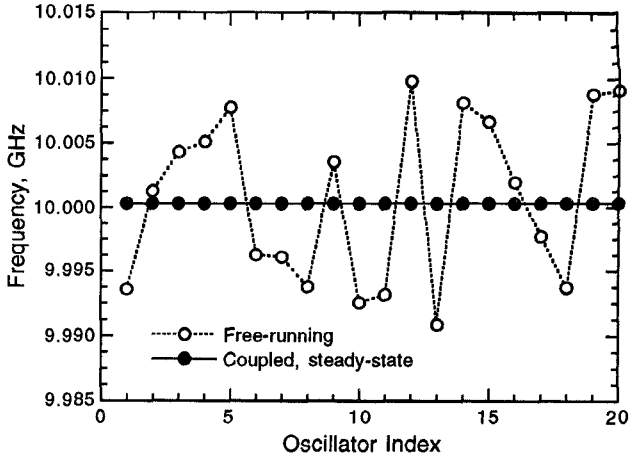


(a)

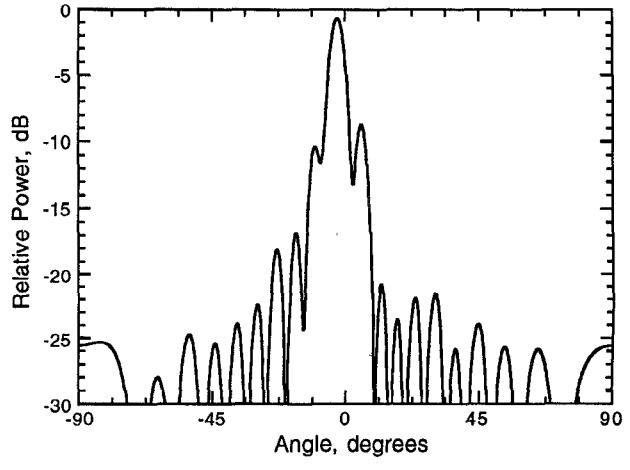


(b)

Fig. 5. Results of a numerical integration of (15) for twenty $X$-band oscillators, with a random free-running frequency distribution and $\Delta\omega_m = 50$ MHz. (a) Oscillator frequencies at the start of the simulation (free running) and after approximately 1 $\mu$s (steady-state), indicating mutual synchronization has occurred. (b) Array factor computed from the steady-state phase relationship.

### D. Beam-Scanning

Since the free-running frequency distribution has such a strong influence on the steady-state phase relationships, it is natural to investigate the possibility of exploiting this effect for beam scanning. In a phased antenna array, the radiation pattern is "steered" in a particular direction by establishing a constant phase progression along the array. For a linear array, steering the beam to an angle $\psi$ off broadside requires a phase shift $\Delta\phi$ between adjacent elements of [45]

$$\Delta\phi = \frac{2\pi d}{\lambda_0}\sin\psi \qquad (36)$$

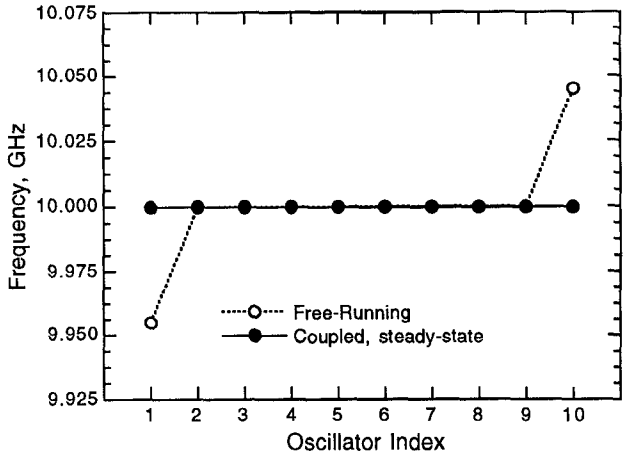


(a)

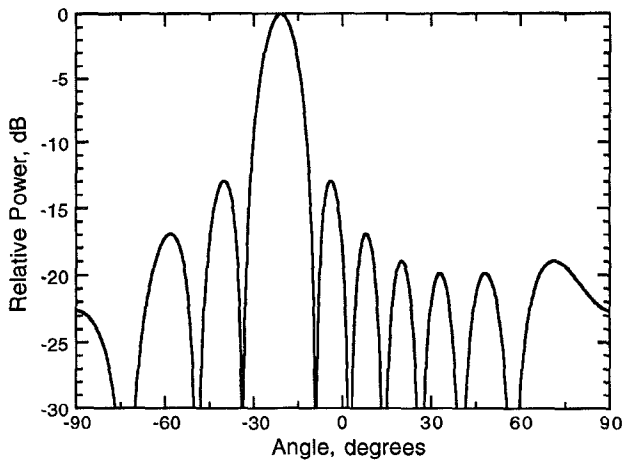


(b)

Fig. 6. Results of a numerical integration of (15) for 10 X-band oscillators, with $\Delta\omega_m = 50$ MHz. (a) Free-running frequencies chosen from (37) lead to (b) a scanned beam as predicted.

where $d$ is the antenna spacing and $\lambda_0$ is the free-space wavelength. Equation (17) can be used to show that a constant phase progression, $\Delta\theta_i = \Delta\phi$, can be achieved by using the frequency distribution

$$\omega_i = \begin{cases} \omega + \Delta\omega_m \sin(\Phi + \Delta\phi) & \text{if } i = 1 \\ \omega + 2\Delta\omega_m \sin\Phi \cos\Delta\phi & \text{if } 1 < i < N \\ \omega + \Delta\omega_m \sin(\Phi - \Delta\phi) & \text{if } i = N. \end{cases} \quad (37)$$

For the case of $\Delta\phi = 0°$, (37) reduces to the frequency distribution (24). Although (37) indicates that any phase shift $\Delta\phi$ can be obtained, a stability analysis puts limits on this quantity. For the special case of $\Phi = 0°$, the limits are $-90° < \phi < 90°$, and the constant phase shift is created by slightly detuning the end elements of the array by equal amounts but in opposite directions. This is illustrated in Fig. 6 for a 10-element array with $\Phi = 0°$ and $\Delta\omega_m = 50$ MHz. The end elements were tuned to $10 \pm 0.045$ GHz, giving $\Delta\phi = -64.2°$. For an array with antenna spacing $d = \lambda_0/2$, this phase shift scans the beam to $\psi \approx -21°$ from broadside, as shown in Fig. 6(b). This new beam-scanning technique is discussed in more depth in another publication [13].

Beam-scanning through control of the end-elements of a coupled oscillator array was also proposed by Stephan [9]–[10], although in different form. In that approach, the first and last oscillators in an array are locked to two external signals which have a prescribed phase difference. This phase difference is then divided equally along the chain. For large arrays, only small phase shifts could be obtained. In contrast, the phase shift obtained with the present method is independent of the number of oscillators. Interestingly, the present situation was also considered in explaining the spinal locomotion of eels and fish [23], where the constant phase progression was interpreted as a travelling wave on the chain, corresponding to swimming action.

## IV. Experimental Results with a Four-Element Array

Although the theory has not yet been exhaustively tested, several published experimental results correlate well with the predictions of the previous sections. These experiments have used a variety of active antenna designs [14]–[19]. In [43], a simple technique was described for characterizing the coupling parameters $\varepsilon$ and $\Phi$ experimentally, and a two-oscillator system was subsequently explored which verified the present theory for that special case. Two $X$-band, $4 \times 4$ active patch arrays using Gunn diodes and MESFET's were also successfully built [3], demonstrating that mutual synchronization can occur with the desired phase distribution in the presence of small random frequency deviations. These arrays were capable of locking to an incident propagating beam, and were shown to degrade gracefully as certain elements were shut down to simulate device failure. A small array of oscillators coupled by one-wavelength transmission lines has also been built [19], demonstrating that in-phase operation is achieved when $\Phi = 0°$. Although a different design methodology was used in the periodic spatial combiner of [7], it can similarly be modelled as a chain of coupled oscillators with $\Phi = 0°$. Most recently, the beam-scanning technique discussed in Section III-D has been verified experimentally using a small chain of four MESFET oscillators [13].

In this section, a few additional results are described using a four-oscillator system which similarly correlate well with the theory. In particular, the influence of the coupling phase $\Phi$ is explored. For the simple case of four oscillators with identical free-running parameters, (19) can be solved analytically giving

$$\overline{\Delta\theta} = \begin{pmatrix} \Delta\theta_1 \\ \Delta\theta_2 \\ \Delta\theta_3 \end{pmatrix} = \begin{pmatrix} \mp\sin^{-1}\left(\frac{1}{2}\tan\Phi\right) \\ 0, \pi \\ -\Delta\theta_1 \end{pmatrix} \quad \text{or}$$
$$\begin{pmatrix} \Phi - \cos^{-1} \pm \sqrt{\frac{4\cos^4\Phi - \sin^2\Phi}{4\cos 2\Phi}} \\ \pm\sin^{-1}[2\sin\Phi\cos(\Phi - \Delta\theta_1)] \\ \pi - 2\Phi + \Delta\theta_1 \end{pmatrix}. \quad (38)$$

These solutions represent eight unique phase distributions, taking account of the various combinations of signs and the multi-valued inverse-trig functions. The stability matrix is given by (39) at the bottom of the next page. Stable solutions have been calculated for several values of $\Phi$, and listed in Table I. The normalized frequency deviation $\Delta\omega/\Delta\omega_m = (\omega - \omega_0)/\Delta\omega_m$

TABLE I
THEORETICAL PHASE DISTRIBUTION IN A FOUR -ELEMENT CHAIN WITH IDENTICAL FREE-RUNNING PARAMETERS, AS A FUNCTION OF THE COUPLING ANGLE $\Phi$.

| | $\Phi = \phi$ | | | | $\Phi = 180° - \phi$ | | | |
|---|---|---|---|---|---|---|---|---|
| $\phi$ | $\Delta\theta_1$ | $\Delta\theta_2$ | $\Delta\theta_3$ | $\frac{\Delta\omega}{\Delta\omega_m}$ | $\Delta\theta_1$ | $\Delta\theta_2$ | $\Delta\theta_3$ | $\frac{\Delta\omega}{\Delta\omega_m}$ |
| 0° | 0° | 0° | 0° | 0% | 180° | 180° | 180° | 0% |
| 10° | -5.1° | 0° | 5.1° | -26.0% | -174.9° | 180° | 174.9° | 26.0% |
| 20° | -10.5° | 0° | 10.5° | -50.7% | -169.5° | 180° | 169.5° | 50.7% |
| 30° | -16.8° | 0° | 16.8° | -72.9% | -163.2° | 180° | 163.2° | 72.9% |
| 40° | -24.8° | 0° | 24.8° | -90.5% | -155.2° | 180° | 155.2° | 90.5% |
| 50° | -36.6° | 0° | 36.6° | -99.8% | -143.4° | 180° | 143.4° | 99.8% |
| 60° | 0°<br>-60° | 60°<br>-60° | 60°<br>0° | -86.6% | 180°<br>-120° | 120°<br>-120° | 120°<br>180° | 86.6% |
| 70° | 11.3°<br>-51.3° | 77.7°<br>-77.7° | 51.3°<br>-11.3° | -85.4% | 168.7°<br>-128.7° | 102.3°<br>-102.3° | 128.7°<br>-168.7° | 85.4% |
| 80° | 20.5°<br>-40.5° | 87.0°<br>-87.0° | 40.5°<br>-20.5° | -86.2% | 159.5°<br>-139.5° | 93.0°<br>-93.0° | 139.5°<br>-159.5° | 86.2% |
| 90° | No Stable Solution | | | | | | | |

is also listed, where $\omega_0$ is the free-running frequency common to each oscillator. Notice that for $\Phi < 60°$ and $\Phi > 120°$, there is only a single stable mode which produces a symmetrical radiation pattern; that is, if the oscillators are numbered in the opposite sequence, the same phase distribution is obtained. However, in the range $60° < \Phi < 120°$, there are two stable modes which correspond to asymmetrical radiation patterns. Since both are stable modes, the mode which actually occurs will be dependent on the initial conditions at startup. This is an interesting result, although clearly undesirable in a practical array, suggesting that coupling angles in this range should be avoided.

A small array of radiatively coupled active patch oscillators was fabricated as shown in Fig. 7. Individual $X$-band Gunn oscillators [14], [15], [18] were mounted on small aluminum carriers, which were then secured to a larger block through a long slot. This slot permitted the carriers to be moved along one dimension, so that the spacing between the oscillators could be varied. Since the coupling parameters in radiatively coupled arrays depends primarily on the antenna separation, the coupling angle could be changed over a wide range using this setup. The coupling parameters were characterized as a function of the oscillator spacing using the technique described in [43]. The oscillators were tuned to a free-running frequency of 11 GHz, and were coupled in the E-plane [43]. The coupling parameters were found to be well approximated by the model $\varepsilon'(x) = A/k_0 x$ and $\Phi(x) = k_0 x + \psi$, where $\varepsilon'(x) \equiv \varepsilon(x)/2Q$, $x$ is the antenna spacing, $k_0$ is the free-space propagation constant, and $A = 0.01$ and $\psi = -80°$.

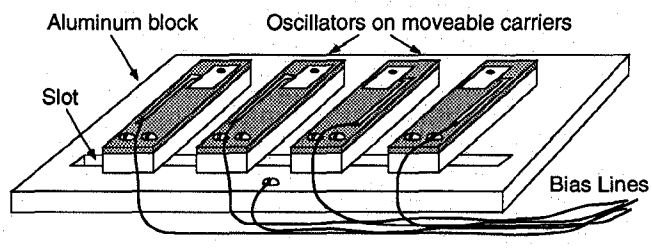


Fig. 7. Illustration of the experimental array used to explore the influence of the coupling angle $\Phi$. $X$-band Gunn oscillators using patch antennas [14] were individually mounted on small aluminum carriers such that the spacing (and hence coupling parameters) could be varied.

Measured radiation patterns, combined with simple array theory [45], offer an excellent means for determining the phase relationship in the array. Measured radiation patterns for three different oscillator spacings of $d = 15, 20$ and 35 mm, corresponding to coupling phase angles of $\Phi = 120°, 180°$, and $360°$, are shown in Fig. 8. Theoretical patterns based on the phase distributions of Table I, a $4 \times 1$ array factor, and a simple patch radiation model [46] are plotted on these graphs for comparison. Elements of the array were found to have nearly identical characteristics, except for one element whose output power was $-3$ dB down from the others; this is accounted for in the theoretical array factor. Good qualitative agreement is observed between theory and experiment regarding the number and placement of lobes and nulls in the patterns, which is a clear indication that the theoretical phase distribution is correct. Discrepancies in magnitude can be partly attributed to the simplistic model used for the patch radiation pattern as well as the deviations in free-running parameters from their assumed values

For the case of $\Phi = 120°$ in Fig. 8(a), Table I indicates that there are two different modes which are mirror images of each other. Only one of these was consistently observed, perhaps because of the slight asymmetry caused by the oscillator with smaller amplitude. Note also that a coupling phase of $\Phi = 0°$ could only be obtained with spacings greater than a wavelength, which explains the grating lobes in Fig. 8(c). As mentioned earlier, this is a common affliction in such radiatively coupled arrays. In the future, methods for increasing the coupling strength and controlling the coupling phase with planar circuitry will be explored.

## V. CONCLUSIONS

A simple theory describing the dynamics of loosely-coupled nonlinear oscillators has been shown to adequately describe the phase relationships in practical arrays. The theory indicates that the free-running frequency distribution has a profound effect on the steady-state phases, as does the coupling phase

$$\overline{\overline{M}} = \begin{pmatrix} -2\cos\Phi\cos\Delta\theta_1 & \cos(\Phi + \Delta\theta_2) & 0 \\ \cos(\Phi - \Delta\theta_1) & -2\cos\Phi\cos\Delta\theta_2 & \cos(\Phi + \Delta\theta_3) \\ 0 & \cos(\Phi - \Delta\theta_2) & -2\cos\Phi\cos\Delta\theta_3 \end{pmatrix}. \tag{39}$$

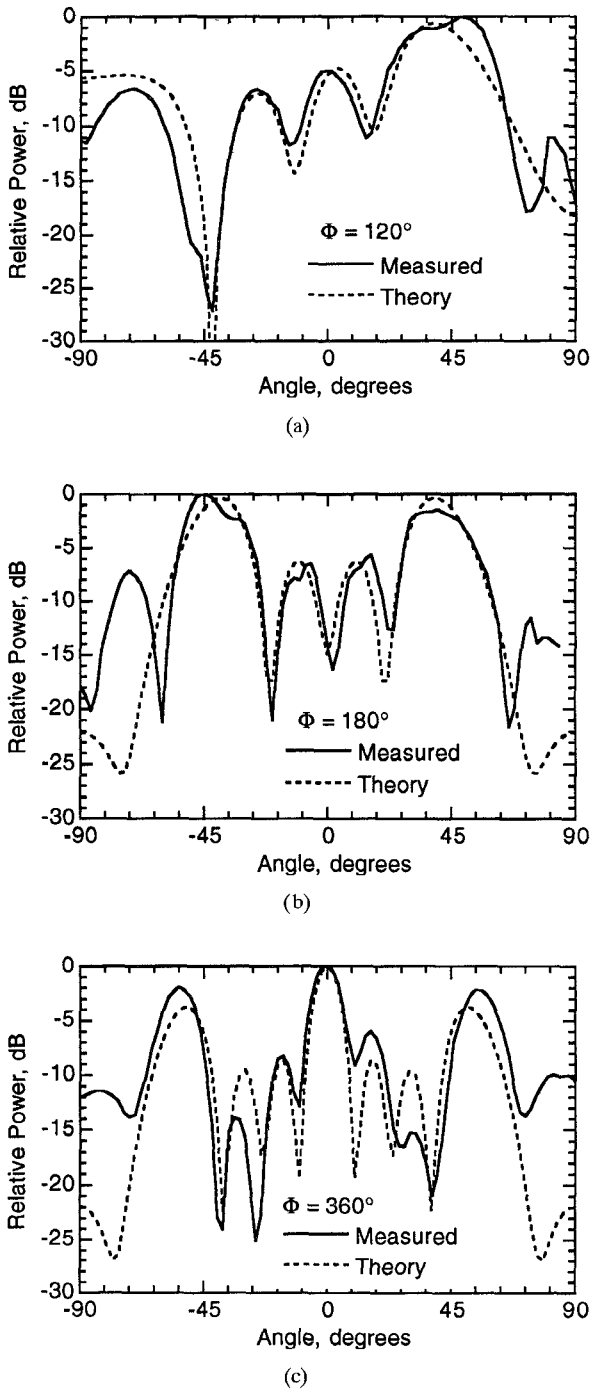


Fig. 8. Measured and theoretical radiation patterns for three different coupling angles. Spacings of (a) 15 mm, (b) 20 mm, and (c) 35 mm produced coupling phases of $\Phi = 120°$, $\Phi = 180°$, and $\Phi = 360°$, respectively, according to the models described in [43]. The theoretical patterns used a simple model for the patch radiation pattern [46].

angle. Frequency distributions for obtaining broadside beams or scanned beams were derived, showing that end elements are primary contributors to the phase relationships. It was also shown that if the frequencies are distributed randomly, there exists a critical value for coupling strength below which no locking can occur. Similarly, a worst-case scan angle deviation can be predicted from the random distribution. Thus a practical array can tolerate a certain amount of randomness as a function of the coupling parameters and design constraints.

This theory will also be useful in exploring other dynamic effects in arrays. Modulation speed is an important criterion which has yet to be investigated, along with the related issue of locking to an external signal, which can be an incident plane wave or a signal directly applied to one oscillator of the system. The noise properties of the array are also of interest, as it is unclear whether the noise of an ensemble of devices will be better or worse than a single device. Locking the array to a low-power, low noise master oscillator may be required. The influence of non-nearest neighbor coupling must also be investigated, since this permits the arrays to degrade gracefully. This includes the use of a Fabry–Perot cavity. The dynamics of two-dimensional arrays were not considered in this paper for notational convenience, but clearly most practical arrays must be two-dimensional to accommodate enough devices. There are also published modifications to the Van der Pol model [33]–[34] which could be used to represent microwave oscillators more realistically. Many of these possibilities are currently under investigation.

## ACKNOWLEDGMENT

The author wishes to acknowledge Dr. J. Mink at ARO, and Professors R. C. Compton at Cornell University and D. B. Rutledge at Caltech for support and encouragement.

## REFERENCES

[1] J. W. Mink, "Quasi-optical power combining of solid-state millimeter-wave sources," *IEEE Trans. Microwave Theory Tech.*, vol. MTT-34, pp. 273–279, Feb. 1986.

[2] D. B. Rutledge, Z. B. Popovic, R. M. Weikle, M. Kim, K. A. Potter, R. A. York, and R. C. Compton, "Quasi-optical power combining arrays," *IEEE MTT-S Int. Microwave Symp. Dig.*, Dallas, May 1990.

[3] R. A. York and R. C. Compton, "Quasi-optical power-combining using mutually synchronized oscillator arrays," *IEEE Trans. Microwave Theory Tech.*, vol. 39, pp. 1000–1009, June 1991.

[4] Z. B. Popovic, R. M. Weikle, M. Kim, and D. B. Rutledge, "A 100-MESFET planar grid oscillator," *IEEE Trans. Microwave Theory Tech.*, vol. 39, pp. 193–200, Feb. 1991.

[5] J. Birkeland and T. Itoh, "A 16 element quasi-optical FET oscillator power combining array with external injection locking," *IEEE Trans. Microwave Theory Tech.*, vol. 40, pp. 475–481, Mar. 1992.

[6] K. Chang, K. A. Hummer, and J. L. Klein, "Experiments on injection-locking of active antenna elements for active phased arrays and spatial power combiners," *IEEE Trans. Microwave Theory Tech.*, vol. 37, pp. 1078–1084, July 1989.

[7] J. Heinbockel and A. Mortazawi, "A periodic spatial power combining MESFET oscillator," *IEEE MTT-S Int. Microwave Symp. Dig.*, Albuquerque, June 1992.

[8] R. J. Dinger, D. J. White, and D. R. Bowling, "10 GHz space power-combiner with parasitic injection-locking," *Electron. Lett.*, vol. 23, pp. 397–398, vol. 9, Apr., 1987.

[9] K. D. Stephan, "Inter-injection-locked oscillators for power combining and phased arrays," *IEEE Trans. Microwave Theory Tech.*, vol. MTT-34, pp. 1017–1025, Oct. 1986.

[10] K. D. Stephan and W. A. Morgan, "Analysis of inter-injection-locked oscillators for integrated phased arrays," *IEEE Trans. Antennas Propagat.*, vol. AP-35, pp. 771–781, July 1987.

[11] R. A. York and R. C. Compton, "Mode-locked oscillator arrays," *IEEE Microwave Guided Wave Lett.*, vol. 1, pp. 215–218, Aug. 1991.

[12] R. A. York and R. C. Compton, "Experimental observation and simulation of mode-locking in coupled-oscillator arrays," *J. Appl. Phys.*, vol. 71, no. 6, pp. 2959–2965, 15 Mar. 1992.

[13] P. Liao and R. A. York, "A new phase-shifterless beam-scanning technique using arrays of coupled oscillators," submitted to *IEEE Trans. Microwave Theory Tech.*, 1992.

[14] H. J. Thomas, D. L. Fudge, and G. Morris, "Gunn source integrated with microstrip patch," *Microwaves & RF*, pp. 87–89, Feb. 1985.

[15] R. A. York and R. C. Compton, "Dual device active patch antenna with improved radiation characteristics," *Electron. Lett.,* vol. 28, pp. 1019–1021, May 1992.
[16] R. A. York, R. M. Martinez, and R. C. Compton, "Hybrid transistor and patch antenna element for array applications," *Electron. Lett.,* vol. 26, pp. 494–495, Mar. 1990.
[17] T. O. Perkins, "Active microstrip circular patch antenna," *Microwave J.,* pp. 110–117, 1987.
[18] K. Chang, K. A. Hummer, and G. K. Gopalakrishnan, "Active radiating element using FET source integrated with microstrip patch antenna," *IEEE Trans. Microwave Theory Tech.,* vol. MTT-31, pp. 91–92, Sept. 1988.
[19] N. Camilleri and B. Bayraktaroglu, "Monolithic millimeter-wave IMPATT oscillator and active antenna," *IEEE Trans. Microwave Theory Tech.,* vol. 36, pp. 1670–1676, Dec. 1988.
[20] N. Wang and S. E. Schwarz, "Monolithically integrated Gunn oscillator at 35 GHz," *Electron. Lett.,* vol. 20, pp. 603–604, July 5, 1984.
[21] I. Peterson, "Step in time: Exploring the mathematics of synchronously flashing fireflies," *Science News,* vol. 140, pp. 136–137, Aug. 1991.
[22] P. C. Matthews and S. H. Strogatz, "Phase diagram for the collective behavior of limit-cycle oscillators," *Phys. Rev. Lett.,* vol. 65, pp. 1701–1704, 1990.
[23] A. H. Cohen, P. J. Holmes, and R. H. Rand, "The nature of the coupling between segmental oscillators of the Lamprey spinal generator for locomotion: A mathematical model," *J. Math. Bio.,* vol. 13, pp. 345–369, 1982.
[24] N. Koppel, "Toward a theory of modelling central pattern generators," *Neural Control of Rhythmic Movements in Vertebrates,* A. H. Cohen, Ed., New York: Wiley, 1988, ch. 10.
[25] J. Buck, *Quart. Rev. Biol.,* vol. 63, p. 265, 1988; T. J. Walker, *Science,* vol. 166, p. 891, 1969; M. K. McClintock, *Nature,* London, vol. 229, p. 224, 1971.
[26] Y. Yamaguchi, K. Komentani, and H. Shimizu, "Self-synchronization of nonlinear oscillations in the presence of fluctuations," *J. Statistical. Phys.,* vol. 26, pp. 719–743, 1981.
[27] P. C. Matthews, R. E. Mirollo, and S. H. Strogatz, "Dynamics of a large system of coupled nonlinear oscillators," *Physica D,* vol. 52, p. 293, 1991.
[28] K. Y. Tsang, R. E. Mirollo, S. H. Strogatz, and K. Wiesenfeld, "Dynamics of a globally coupled oscillator array," *Physica D,* vol. 48, pp. 102–112, 1991.
[29] G. B. Ermentrout and N. Kopell, "Frequency plateaus in a chain of weakly coupled oscillators, I.," *SIAM J. Math Anal.,* vol. 15, pp. 215–237, 1984.
[30] N. Kopell and G. B. Ermentrout, "Symmetry and phaselocking in chains of weakly coupled oscillators," *Comm. Pure Appl. Math,* vol. 39, pp. 623–660, 1986.
[31] S. H. Strogatz and R. E. Mirollo, "Phase-locking and critical phenomena in lattices of coupled nonlinear oscillators with random intrinsic frequencies," *Physica D,* vol. 31, pp. 143–168, 1988.
[32] B. Van der Pol, "The nonlinear theory of electric oscillations," *Proc. IRE,* vol. 22, pp. 1051–1085, Sept. 1934.
[33] K. Fukumoto, M. Nakajima, and J.-I. Ikenoue, "Mathematical representation of microwave oscillator characteristics by use of the Rieke diagram," *IEEE Trans. Microwave Theory Tech.,* vol. MTT-31, pp. 954–959, Nov. 1983.
[34] K. Fukumoto, M. Nakajima, and J.-I. Ikenoue, "Mathematical expression of the loading characteristics of microwave oscillators and injection-locking characteristics," *IEEE Trans. Microwave Theory Tech.,* vol. MTT-33, pp. 319–323, Apr. 1985.
[35] R. Adler, "A study of locking phenomena in oscillators," *Proc. IRE,* vol. 34, pp. 351–357, June 1946; also reprinted in *Proc. IEEE,* vol. 61, pp. 1380–1385, Oct. 1973.
[36] K. Kurokawa, "Injection-locking of solid-state microwave oscillators," *Proc. IEEE,* vol. 61, pp. 1386–1409, Oct. 1973.
[37] A. E. Siegman, *Lasers,* University Science Books, California, 1986.
[38] S. Wiggins, *Introduction to Nonlinear Dynamical Systems and Chaos.* Berlin: Springer, 1990.
[39] F. Verhulst, *Nonlinear Differential Equations and Dynamical Systems.* Berlin: Springer, 1990.
[40] C. R. Wylie and L. C. Barrett, *Advanced Engineering Mathematics, 5th ed.,* New York: McGraw Hill, 1982.
[41] G. H. Gloub and C. F. Van Loan, *Matrix Computations, 2nd ed.,* Baltimore: Johns Hopkins Press, 1989.
[42] W. P. Shillue and K. D. Stephan, "A technique for the measurement of mutual impedance of monolithic solid-state quasi-optical oscillators," *Microwave and Optical Tech. Lett.,* Dec. 1990.
[43] R. A. York and R. C. Compton, "Measurement and modelling of radiative coupling in oscillator arrays," to appear in *IEEE Trans. Microwave Theory Tech.,* vol. MTT-41, pp. 438–444, Mar. 1993.
[44] Press *et al., Numerical Recipes,* New York: Cambridge University Press, 1989.
[45] W. L. Stutzman and G. A. Thiele, *Antenna Theory and Design.* New York: Wiley, 1981.
[46] J. R. James, P. S. Hall, C. Wood, *Microstrip Antenna Theory and Design.* London: Peter Peregrinus Ltd., 1981, pp. 77–80.

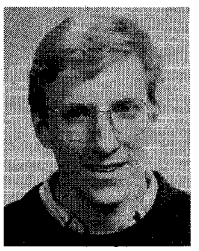

**Robert A. York** (S'86–M'91) received the BS degree in electrical engineering from the University of New Hampshire in 1987, and the MS and Ph.D. degrees in electrical engineering at Cornell University in 1989 and 1991, respectively.

In November 1991 he joined the faculty of Electrical and Computer Engineering at the University of California at Santa Barbara. His group at UCSB is currently involved with the design and fabrication of microwave and millimeter-wave circuits and devices, quasi-optical device arrays and other nonlinear or non-reciprocal components, and quasi-optical measurement techniques. Dr. York is a member of the Compound Semiconductor Research Group (CO-SEARCH) and the NSF Center for High-Speed Image Processing (CHIP) at UCSB. His other research interests include microwave materials measurements, and developing CAD tools for educational purposes. Dr. York was recipient of a 1990 MTT-S Graduate Fellowship Award, and co-recipient of the Ban Dasher award for best paper at the 1989 IEEE Frontiers in Education Conference. He received an Army Research Office Young Investigator award in 1993.